

**Title: Redefining Nephrotic Syndrome in Molecular Terms:
Outcome-associated molecular clusters and patient stratification with noninvasive
surrogate biomarkers**

Laura H. Mariani^{1*†}, Sean Eddy^{1†}, Sebastian Martini¹, Felix Eichinger¹, Brad Godfrey¹, Viji Nair¹, Sharon G. Adler², Gerry B. Appel³, Ambarish Athavale⁴, Laura Barisoni⁵, Elizabeth Brown⁶, Dan C. Cattran⁷, Katherine M. Dell⁸, Vimal Derebail⁹, Fernando C. Fervenza¹⁰, Alessia Fornoni¹¹, Crystal A. Gadegbeku¹², Keisha L. Gibson⁹, Deb Gipson¹, Lawrence A. Greenbaum¹³, Sangeeta R. Hingorani¹⁴, Michelle A. Hlandunewich¹⁵, John Hogan¹⁶, Larry B. Holzman¹⁶, J. Ashley Jefferson¹⁷, Frederick J. Kaskel¹⁸, Jeffrey B. Kopp¹⁹, Richard A. Lafayette²⁰, Kevin V. Lemley²¹, John C. Lieske¹⁰, Jen-Jar Lin²², Kevin E. Myers²³, Patrick H. Nachman²⁴, Cindy C. Nast², Alicia M. Neu²⁵, Heather N. Reich⁷, Kamal Sambandam⁶, John R. Sedor⁸, Christine B. Sethna²⁶, Tarak Srivastava²⁷, Howard Trachtman²⁸, Cheryl Tran¹⁰, Chia-shi Wang¹³, Matthias Kretzler^{1*}

Affiliations:

¹Michigan Medicine, Ann Arbor, MI, USA

²Harbor-UCLA Medical Center, Torrance, CA, USA

³Columbia University, New York, NY, USA

⁴John H Stroger Jr. Hospital of Cook County, Chicago, IL, USA

⁵Duke University School of Medicine, Durham, NC, USA

⁶UT Southwestern Medical Center, Dallas, TX, USA

⁷University Health Network, Toronto, ON, Canada

⁸Cleveland Clinic, Cleveland, OH, USA

⁹University of North Carolina, Chapel Hill, NC, USA

¹⁰Mayo Clinic, Rochester, MN, USA

¹¹University of Miami Health System, Miami, FL, USA

¹²Temple University School of Medicine, Philadelphia, PA, USA

¹³Emory University School of Medicine and Children's Healthcare of Atlanta, Atlanta, GA, USA

¹⁴Seattle Children's Hospital, Seattle, WA, USA

¹⁵Sunnybrook Hospital, University Health Network, University of Toronto, Toronto, ON, Canada

¹⁶Penn Medicine, Philadelphia, PA, USA

¹⁷University of Washington Medicine, Seattle, WA, USA

¹⁸Montefiore Medical Center, Bronx, NY, USA

¹⁹National Institute of Diabetes and Digestive and Kidney Diseases, Bethesda, MD, USA

²⁰Stanford University Medical Center, Stanford, CA, USA

²¹Children's Hospital of Los Angeles, Los Angeles, CA, USA

²²Wake Forest School of Medicine, Winston-Salem, NC, USA

²³Children's Hospital of Philadelphia, Philadelphia, PA, USA

²⁴University of Minnesota, Minneapolis, MI, USA

²⁵ Johns Hopkins University, Baltimore, MD, USA

²⁶ Northwell Health, New Hyde Park, NY, USA

²⁷ Children's Mercy Hospital, Kansas City, MO, USA

²⁸ NYU Langone Health, New York, NY, USA

To whom correspondence should be addressed: include the email addresses of the corresponding author(s). Please use the asterisk () symbol for the corresponding author information.

† Co-first authors

Summary: A tissue transcriptome driven classification of nephrotic syndrome patients identified a high risk group of patients with TNF activation and established a non-invasive marker panel for pathway activity assessment paving the way towards precision medicine trials in NS.

Abstract: Nephrotic syndrome from primary glomerular diseases can lead to chronic kidney disease (CKD) and/or end-stage renal disease (ESRD). Conventional diagnoses using a combination of clinical presentation and descriptive biopsy information do not accurately predict risk for progression in patients with nephrotic syndrome, which complicates disease management. To address this challenge, a transcriptome-driven approach was used to classify patients with minimal change disease and focal segmental glomerulosclerosis in the Nephrotic Syndrome Study Network (NEPTUNE). Transcriptome-based classification revealed a group of patients at risk for disease progression. High risk patients had a transcriptome profile consistent with TNF activation. Non-invasive urine biomarkers TIMP1 and CCL2 (MCP1), which are causally downstream of TNF, accurately predicted TNF activation in the NEPTUNE cohort setting the stage for patient stratification approaches and precision medicine in kidney disease.

Introduction

Nephrotic syndrome (NS) refers to a glomerular disease with a shared clinical presentation, which is marked by proteinuria, hypoalbuminemia, hyperlipidemia and edema which can ultimately lead to kidney failure. Several underlying diseases can result in this constellation of symptoms, including the primary glomerular diseases of minimal change disease (MCD) and focal segmental glomerulosclerosis (FSGS), currently classified by the descriptive pattern of injury seen on kidney biopsy. Although these primary glomerular diseases are categorized as distinct histopathologic categories, they likely result from heterogeneous biological processes given the person to person variability in disease onset, rates of progression and response rates to various immunosuppressive therapies (1). Currently, diagnostic, prognostic and therapeutic decisions are based on these histopathologic categories and routine clinical parameters (e.g. serum creatinine and urine protein) that do not account for the heterogeneity of the biological antecedents. Because of the imprecise diagnosis within the current descriptive disease classification, molecularly targeted treatments for these diseases are not routinely available, and the interpretation of results from observational studies and clinical trials of therapeutic agents, which enroll a heterogeneous population of NS patients, are difficult to interpret. In such studies, it is often observed while the overall trial reads out negative, a small subset of patients respond well to the trialed therapy (2-6), yet pre-treatment predictors of response are not available.

Advances in biomedical research allow for capture of high-dimensional data across the genotype-phenotype continuum from patients under routine clinical care and can serve as a platform for implementation of precision medicine within NS (7). This approach utilizes large scale data integration across multiple data domains paired with deep clinical phenotype to establish a disease classification which is based in molecular causes as well as clinical presentation. Ultimately, the overarching goal of this approach is to assign targeted treatment based on these refined diagnostic categories which can reliably be identified using non-invasive markers (Figure 1).

Kidney diseases are uniquely positioned to implement this approach as a kidney biopsy is the diagnostic gold standard for NS, allowing for identification of molecular tissue signatures which can be linked to detailed histopathology assessment and non-invasive urine markers and validated against clinical outcome. In this study, we utilize the prospective Nephrotic Syndrome Study Network (NEPTUNE) cohort and its European sister network (European Renal cDNA Bank (ERCB)) to implement this approach and identify a sub group of patients with a shared molecular signature, potentially amenable to targeted therapy.

Results

Unbiased Hierarchical Clustering of Tubulointerstitial Compartment Gene Expression to Identify Molecular Subgroups of Nephrotic Syndrome: 123 NEPTUNE patients with MCD and FSGS were clustered into three groups (n=62, 42, and 19, respectively) according to their tubulointerstitial mRNA expression levels from their clinically-indicated renal biopsy (Supplemental Figure 1). Baseline characteristics of the participants in each cluster are listed in table 1. Patients in cluster three were older, and had lower eGFR and higher UPCR at baseline. There was no difference in race, sex or duration of disease across the clusters. Although cluster 3 had a greater proportion with FSGS, all three clusters had participants with both MCD and FSGS according to the conventional histopathologic classification. In an unadjusted survival model, Cluster 3 had a more progressive phenotype, with lower hazard of complete remission (p-value 0.002) and greater hazard of the composite of ESRD or 40% decline in eGFR from baseline (p-value 0.007, Figure 2).

Functional context of differentially expressed genes and replication in independent cohort: 2517 genes were differentially regulated in the NEPTUNE cohort between cluster 3 versus 1 and 2, with a 1.5 fold-change and q-value <0.05. TNF itself was increased and found to center one of the top gene interaction networks from the differentially expressed gene set (Figure 3A). Genes were further analyzed to determine functional context of elevated TNF expression in Cluster 3. The canonical signal transduction pathways with the highest enrichment score was granulocyte adhesion and diapedesis with 54 of 151 (35.8%) pathway genes differentially expressed in cluster 3 (p-value<0.001). Differentially expressed genes in this pathway included TNF, which was one of the pathway activation inputs. In upstream regulator analysis (an analysis that takes into account both enrichment of and underlying direction of differential gene expression changes using cause and effect relationships), the top predicted activated protein network was TNF (IPA Z-score=10.2, enrichment p-value=3.65E-84, Figure 3B). A mechanistic network centered on downstream effects of TNF activation explained 26% (660/2517) of the differentially expressed genes in the analysis and included multiple transcription factors previously implicated in chronic kidney diseases including activation of the NFκB complex (as well as activation of NFκB1 (p105/p50) and RELA (p65) subunits) (8-10), and STAT1 and STAT3 (11). Lastly, 11 of the genes in the TNF causal network (including *TNF*) were supported by multiple literature assertions in IPA (Figure 3C), and were also profiled on a targeted proteomic profile panel.

To validate the molecular profiles identified in this cluster, unsupervised hierarchical clustering was applied to an independent cohort. Tubulointerstitial transcriptome data from 30 patients with MCD and FSGS in the European Renal cDNA Bank (ERCB) was used for validation (Supplementary Table 1). As in the NEPTUNE discovery cohort and three clusters were also identified. Patients in the ERCB cluster 3 also had significantly lower mean eGFR (35 ± 17 , n=6, p<0.001) compared to the other two clusters (94 ± 35 for the combined cluster 1 and 2, also see Supplementary Table 1). A differential expression

analysis was also performed between cluster 3 and the other clusters. Genes that met a q -value <0.05 threshold in both NEPTUNE and ERCB displayed a high correlated expression profile (Supplemental Figure 2, R^2 of $\text{Log}_2\text{FC} = 0.84$, $p < 0.001$, with 93% of transcripts sharing directionality of change). To further validate the NEPTUNE findings, the same differential expression filter was applied (1.5 fold-change and q -value <0.05) to the ERCB cohort cluster 3 signature. This resulted in 703 genes and consistent with the findings from the NEPTUNE cohort, the top predicted protein network was activation of TNF (IPA Z-score=7.2, p -value=1.9E-22). Predicted activation of TNF explained 23% (163/703) of the differentially expressed genes in this cohort.

Patient-level TNF score and relationship with cluster: To be able to quantify TNF activation within individual patient samples, and assess its association with NS cluster assignment, a TNF activation score was generated using causal assertions were associated with predicted TNF activation in the NEPTUNE cohort. Starting with 398 genes that contributed to predicted TNF activation, genes were limited to those with multiple (≥ 3) lines of curated literature evidence (to limit spurious associations), and then further to those up-regulated by TNF (as a majority of genes ($>95\%$) contributing to predicted TNF activation were up-regulated). This reduced the set of TNF-regulated genes to 145 (Supplementary Table 2). First, Log_2 gene expression data for the 145 genes were converted to Z-scores across the NEPTUNE transcriptomic dataset. Next, the mean of each of the 145 Z-score gene expression values from each participant's profile as the TNF activation score. Participants in cluster 3 had higher TNF activation scores than those in clusters 1 or 2. Mean (SD) score in cluster 3 was 1.01 (0.50), as compared to 0.01 (0.34) in cluster 2 and -0.53 (0.27) in cluster 1, p -value < 0.01 (Figure 4). To address the potential for data overfitting, the 145 gene set was scored in a similar manner in the ERCB cohort. Consistent with differential gene expression profiles, and similar networks identified in the ERCB cohort, the association of TNF activation score with cluster 3 was confirmed in these samples (data not shown). Thus, a molecular signal consistent with TNF activation in primary NS was represented by a downstream gene signature in multiple cohorts.

Association of TNF activation score with clinical outcomes: At baseline, TNF activation score was correlated with severity of interstitial fibrosis ($\rho = 0.69$, p -value < 0.001 , Figure 5), but median (IQR) was 22.5 (10.5 – 49.5) and range was 0 to 71%. To evaluate to what extent TNF activation score from the renal tissue expression data captured the variability in loss of eGFR over time observed in cluster 3 as compared to clusters 1 and 2, a generalized estimating equation (GEE) model of eGFR over time was fit separately with cluster membership and TNF activation score as primary predictors of interest. After adjustment for demographics, diagnosis, time, baseline eGFR and UPCR, cluster 3 was associated with a 19 mL/min/1.73m² lower eGFR during follow-up as compared to cluster 1. Cluster 2 was not significantly different from cluster 1. Similarly, in the fully adjusted model, a 1 unit greater TNF activation score was associated with a 12 mL/min/1.73 m² lower eGFR during follow-up (Table 2).

Non-invasive biomarker identification of TNF activation score: Taking advantage of targeted proteomic data sets available as part of the multi-scalar data platform in NEPTUNE, profiles from 54 urinary cytokines, matrix metalloproteinases and tissue inhibitor of metalloproteinases were investigated. As shown in Figure 3C, 11 proteins with urine biomarker profiles were also part of a TNF causal network (i.e. gene expression values were downstream of TNF and a readout or signature of potential TNF activation in the kidney). Thus, we hypothesized that a biomarker or group of urine biomarkers might be sufficient to recapitulate intra-renal TNF activation and act as non-invasive surrogate biomarkers. Biomarkers with expression profiles in the dynamic range in at least 75% of samples, and those with a high level of intra-renal log₂ mRNA versus log₁₀ urine protein (normalized to creatinine) correlation ($p < 0.0001$, $r^2 \geq 0.25$) in MCD and FSGS were chosen as potentially representative of the intra-renal transcriptional state (Figure 6A). Two genes, *CCL2* and *TIMP1* had corresponding urine proteomic profiles meeting these criteria (Figure 6B). Urine biomarker profiles for *CCL2* (also known as MCP1) and *TIMP1* were highly correlated with the TNF activation score ($p < 0.0001$, $r^2 \geq 0.25$ for both biomarkers, Figure 6C). Thus, these biomarkers were identified as non-invasive surrogates reflective of the intra-renal transcriptional state and of the TNF activation score.

Predictive ability of biomarkers: The base model presented here used eGFR and UPCR and additional models added the urinary biomarker levels of *TIMP1* and *MCP1*. The fully adjusted model had highest c-statistic and positive predictive value for non-invasive assessment of the TNF activation score (Table 3).

Discussion

This work introduces the concept of how a precision medicine strategy can work for nephrotic syndrome. The study utilized kidney biopsy tissue transcriptomics to identify a subgroup of nephrotic syndrome patients with a shared molecular profile and poor clinical outcome. Using an unbiased analysis of tubulointerstitial compartment gene expression data, without clinical or pathology data, a subgroup of participants was identified that had less remission of proteinuria and more loss of kidney function over time. The molecular profile of this group was evaluated for its underlying biological processes and found to center on TNF activation. TNF activation, quantified within individual patients, was sufficient to capture association with poor clinical outcome observed by cluster assignment. A combination of clinical features and urinary biomarkers could then be identified as non-invasive predictors of tissue TNF activation with high accuracy.

TNF is a pro-inflammatory, immunoregulatory cytokine, implicated in many systemic inflammatory diseases as well as kidney diseases (12-14). It is produced by infiltrating immune cells, but also by renal tissue cells, including podocytes and mesangial cells (15). In isolated rat glomeruli, TNF-alpha administration increased albumin permeability (16). In rats that spontaneously develop nephrotic syndrome and FSGS (Buffalo/Mna), renal expression of TNF increases before the onset of proteinuria (17). In humans, TNF levels from cultured peripheral blood mononuclear cells were higher in children with active nephrotic syndrome, compared to those in remission and controls (18). Case reports and small studies have reported that anti-TNF therapy may be effective in a subset of nephrotic syndrome patients, but no data was available on intra-renal activation of the pathway (19-21). Current clinical practice and diagnostic evaluation cannot identify this subset for targeted interventional trials.

Based on this animal and human evidence, the FONT trial (novel therapies in resistant FSGS) tested the TNF inhibitor adalimumab in patients with therapy-resistant FSGS using an unstratified approach (4). Of the total 16 patients treated in the phase I and phase II studies, 2 participants had dramatic improvements in proteinuria (from 17 to 0.6mg/mg and from 3.6 to 0.6 mg/mg in the other). Although the study is considered an unsuccessful trial in demonstrating efficacy of this therapy for all FSGS patients, a response in any of the patients with this severe phenotype is notable. This highlights the biologic heterogeneity underlying the recruited population to this study and similar clinical trials in FSGS. The observation of highly variable and unpredictable response to TNF blockade in the FONT trial is similar to that observed in routine clinical practice to standard therapies. It demonstrates the need for a precision approach to better assign patients to conventional therapies as well as offering access to experimental therapies in the setting of clinical trials to match patients to the most effective medication and sparing toxicity from unnecessary medications.

The pipeline described in this paper could be applied to clinical trial design whereby a nephrotic syndrome population could be enriched for patients with a higher probability of having a particular pathway upregulated and amenable to targeted therapy. Specifically, the coefficients from a validated logistic model could be used to calculate a probability of pathway activation as inclusion criteria for entry

into a clinical trial. Thus, this would increase the chance that a trial would include a higher proportion of patients with a more homogeneous molecular profile amenable to the investigational target.

Several limitations of this approach are acknowledged. The clustering was done using the tubulointerstitial compartment as opposed to the glomerular compartment which is certainly also relevant to the pathophysiology of glomerular diseases. However, tubulointerstitial damage and fibrosis has been shown to be one of the strongest predictors of clinical outcome in the NEPTUNE cohort and treatment response (22), which crosses the conventional disease classifications. Medications targeting this common mechanism may be expected to have efficacy as disease modifying drugs in chronic kidney disease across multiple conventionally diagnosed renal diseases (9). For some patients, high TNF activation may represent a disease too advanced to be amenable to any therapy. However, the analysis did include samples from multiple patients with low interstitial fibrosis and high TNF scores. Bulk expression data was utilized and so differentially expressed genes may reflect differences in cell composition between the clusters. The accuracy of the non-invasive surrogates as dynamic, i.e. target engagement biomarkers requires validation and is being pursued in a proof of concept clinical trial under development.

In conclusion, this study implements a novel pipeline not previously applied in nephrotic syndrome patients to utilize tissue transcriptomics to identify a subgroup of patients with poor clinical outcomes. The potentially targetable pathway, TNF, was identified as a primary driver of disease and non-invasive markers could identify a patient population enriched for TNF activation. This mechanistic based disease classification is the first step to achieving the goal of assigning patients to therapies in a targeted manner and thus minimizing toxicity and maximizing benefit.

Materials and Methods

Study Participants: The study was conducted on 123 participants with biopsy proven Minimal Change Disease (MCD) and Focal Segmental Glomerulosclerosis (FSGS) enrolled in the NEPTUNE study and who had tissue genome wide mRNA expression profiling completed. NEPTUNE is a multi-center, prospective study of children and adults with >500mg/day of proteinuria, recruited at the time of first clinically indicated baseline renal biopsy. Pathologic diagnosis is confirmed by review of digital whole slide images by study pathologists (23). Patients with evidence of other renal disease (e.g., lupus, diabetic nephropathy), prior solid organ transplant, and life expectancy < 6 months were excluded. The study enrolled at 21 clinical sites starting in August, 2010. The objectives and study design of NEPTUNE have been previously described (24) and can be found in the clinicaltrials.gov database under NCT1209000. Consent was obtained from individual patients at enrollment, and the study was approved by Institutional Review Boards of participating institutions. A subset of participants from the European Renal cDNA Cohort (ERCB) (n=30) with MCD and FSGS were used as a validation cohort for the gene expression analyses (25).

Clinical Data: NEPTUNE participants are followed prospectively, every 4 months for the first year, and then biannually thereafter for up to 5 years. Detailed information regarding socio-demographics, medical history and medication exposure are collected by subject interview and chart review. Local laboratory results are recorded and blood and urine specimens are collected at baseline and in each follow-up visit for central measurement of serum creatinine and urine protein/creatinine ratio. eGFR (mL/min/1.73m²) was calculated using the CKD-Epi formula for participants ≥ 18 years old and the modified CKiD-Schwartz formula for participants < 18 years old. ESRD was defined as initiation of dialysis, receipt of kidney transplant or eGFR < 15 mL/min/1.73m² for two measurements. Complete remission was defined as UPCR < 0.3 mg/mg on either a single void specimen or 24-hour urine collection. ERCB is a European multicenter study capturing renal biopsy tissue for gene expression profiling along with cross-sectional clinical information (e.g., demographics, eGFR) collected at the time of a clinically indicated renal biopsy(25).

Molecular Data and Analysis: Genome wide transcriptome analysis was performed on manually micro-dissected renal biopsy tissue that separated the tubulointerstitial compartment from the glomerular compartment. Total RNA was isolated, reverse transcribed, linearly amplified and hybridized on an Affymetrix 2.1 ST platform (NEPTUNE) and U133 platform (ERCB) as described previously (9, 26-29). Gene expression was normalized, log-2 transformed and batch corrected with Entrez Gene ID annotations. Only genes expressed 1 standard deviation above the negative control were considered to be expressed and included in the analysis. Unsupervised hierarchical clustering and differential gene expression analysis was performed with Multiple Experiment Viewer (WebMeV, mev.tm4.org) using the tubulointerstitial compartment expression data. Differentially expressed genes between clusters of interest were analyzed for enrichment of canonical pathways and functional groups using the Ingenuity Pathway Analysis Software Suite (IPA).

TNF Score: Genes causally linked downstream of TNF were selected to compose a TNF activation score.(30) Selected genes were significantly up-regulated (≥ 1.5 -fold change and $q < 0.05$) in the differential expression gene set in cluster 3 compared to 1 and 2 and were predicted to be activated by TNF from 3 independent lines of evidence (i.e. literature references supporting the relationship) from IPA. 145 genes met these criteria (Supplemental table 3) and a z-score was generated for each gene for each patient. The individual z-scores across all 145 genes were averaged to calculate the composite TNF alpha activation score for each patient.

Urine Biomarkers: A panel of 54 urinary cytokines, matrix metalloproteinases and tissue inhibitor of metalloproteinases was available on a subset of NEPTUNE participants using the multiplex Luminex platform. All urine protein levels were normalized to urine creatinine. To be evaluated as a potential non-invasive marker of TNF activation, the urine protein had to be a product of a gene causally linked

downstream of TNF and to be correlated with intra-renal tissue gene expression and TNF activation score.

Statistical Analysis of the Association with Clinical data and Urine Biomarkers: Descriptive statistics, including mean and standard deviation (SD) for normally distributed variables, median and interquartile range (IQR) for skewed variables and proportions for categorical variables were used to characterize baseline participant characteristics by molecular cluster. Multi-variable linear generalized estimating equations (GEE) were used to assess association of molecular cluster and TNF score with eGFR during follow-up. Pearson's correlation was used to assess the relationship between TNF score and urinary biomarker concentration or mRNA expression. Urinary biomarker levels were divided by urinary creatinine to correct for urinary concentration/dilution and were log₂ transformed to achieve a normal distribution. Logistic regression models were fit to assess the association of urinary biomarkers with a positive vs. negative TNF score. C-statistics were calculated from the logistic models to characterize the discrimination of the models. The improved predictive value of urinary biomarkers was assessed using the LR test for nested models. Analyses were performed using STATA, v12.1 (College Station, TX) with two-sided tests of hypotheses and p-value <0.05 as the criterion for statistical significance.

Acknowledgement:

The Nephrotic Syndrome Study Network Consortium (NEPTUNE), U54-DK-083912, is a part of the National Institutes of Health (NIH) Rare Disease Clinical Research Network (RDCRN), supported through collaboration between the Office of Rare Diseases Research, National Center for Advancing Translational Sciences and the National Institute of Diabetes, Digestive, and Kidney Diseases. Additional funding and/or programmatic support for this project has also been provided by the Else Kröner-Fresenius Foundation (ERCB), University of Michigan, the NephCure Kidney International and the Halpin Foundation, and the Applied Systems Biology Core at the University of Michigan George M. O'Brien Kidney Translational Core Center.

Members of the Nephrotic Syndrome Study Network (NEPTUNE)

NEPTUNE Enrolling Centers

Case Western Reserve University, Cleveland, OH: J Sedor^{*}, K Dell^{**}, M Schachere[#], J Negrey

Children's Hospital, Los Angeles, CA: K Lemley^{*}, L Whitted[#]

Children's Mercy Hospital, Kansas City, MO: T Srivastava^{*}, C Haney[#]

Cohen Children's Hospital, New Hyde Park, NY: C Sethna^{*}, K Grammatikopoulos[#], R Odusayana

Columbia University, New York, NY: G Appel^{*}, M Toledo[#]

Emory University, Atlanta, GA: L Greenbaum^{*}, C Wang^{**}, B Lee[#]

Harbor-University of California Los Angeles Medical Center: S Adler^{*}, C Nast[‡], J La Page[#]

John H. Stroger Jr. Hospital of Cook County, Chicago, IL: A Athavale^{*}

Johns Hopkins Medicine, Baltimore, MD: A Neu^{*}, S Boynton[#]

Mayo Clinic, Rochester, MN: F Fervenza^{*}, M Hogan^{**}, J Lieske^{*}, V Chernitskiy[#]

Montefiore Medical Center, Bronx, NY: F Kaskel^{*}, N Kumar^{*}, P Flynn[#]

NIDDK Intramural, Bethesda MD: J Kopp^{*}, E Castro-Rubio[#], J Blake[#]

New York University Medical Center, New York, NY: H Trachtman^{*}, O Zhdanova^{**}, F Modersitzki[#], S Vento[#]

Stanford University, Stanford, CA: R Lafayette^{*}, K Mehta[#]

Temple University, Philadelphia, PA: C Gadegbeku^{*}, D Johnstone^{**}, S Quinn-Boyle

University Health Network Toronto: D Cattran^{*}, M Hladunewich^{**}, H Reich^{**}, P Ling[#], M Romano[#]

University of Miami, Miami, FL: A Fornoni^{*}, L Barisoni^{*}, C Bidot[#]

University of Michigan, Ann Arbor, MI: M Kretzler^{*}, D Gipson^{*}, A Williams[#], R Pitter[#]

University of North Carolina, Chapel Hill, NC: V Derebail^{*}, K Gibson^{*}, S Grubbs[#], A Froment[#]

University of Pennsylvania, Philadelphia, PA: L Holzman^{*}, K Meyers^{**}, K Kallem[#], A Swensen[#]

University of Texas Southwestern, Dallas, TX: K Sambandam^{*}, E Brown^{**}, M Cruz[#]

University of Washington, Seattle, WA: A Jefferson^{*}, S Hingorani^{**}, K Tuttle^{**§}, L Curtin[#], S Dismuke[#], A Cooper^{#§}

Wake Forest University, Winston-Salem, NC: B Freedman^{*}, JJ Lin^{**}, S Gray[#]

Data Analysis and Coordinating Center: M Kretzler, L Barisoni, C Gadegbeku, B Gillespie, D Gipson, L Holzman, L Mariani, M Sampson, P Song, J Troost, J Zee, E Herreshoff, S Li, C Lienczewski, T Mainieri, M Wladkowski, A Williams, D Zinsser

National Institute of Diabetes and Digestive and Kidney Diseases (NIDDK) Program Office: K Abbott, C Roy

The National Center for Advancing Translational Sciences (NCATS) Program Office: T Urv, PJ Brooks

^{*}Principal Investigator; ^{**}Co-investigator; [#]Study Coordinator

[‡]Cedars-Sinai Medical Center, Los Angeles, CA

[§]Providence Medical Research Center, Spokane, WA

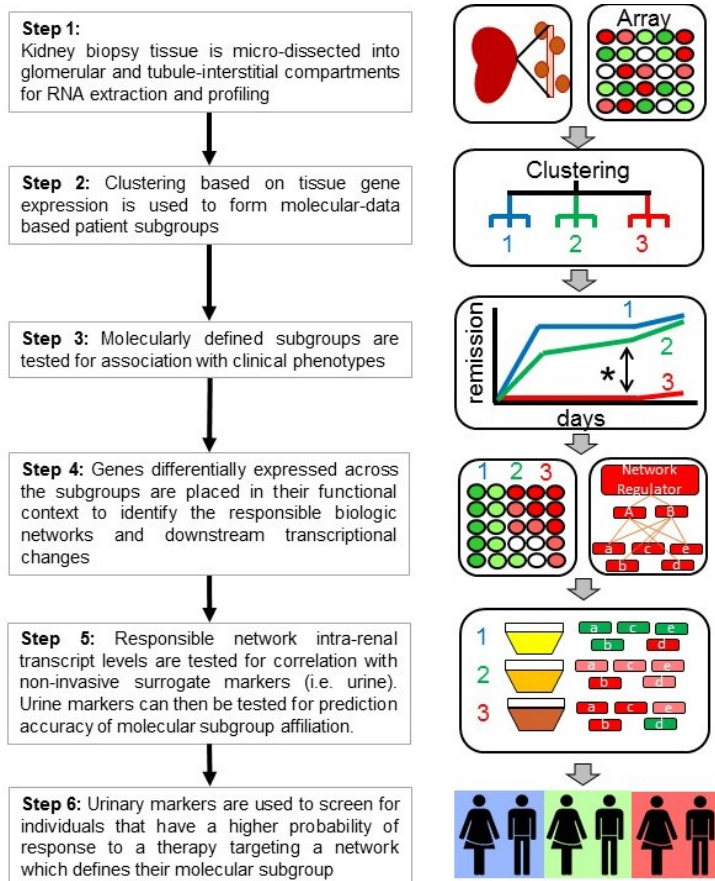
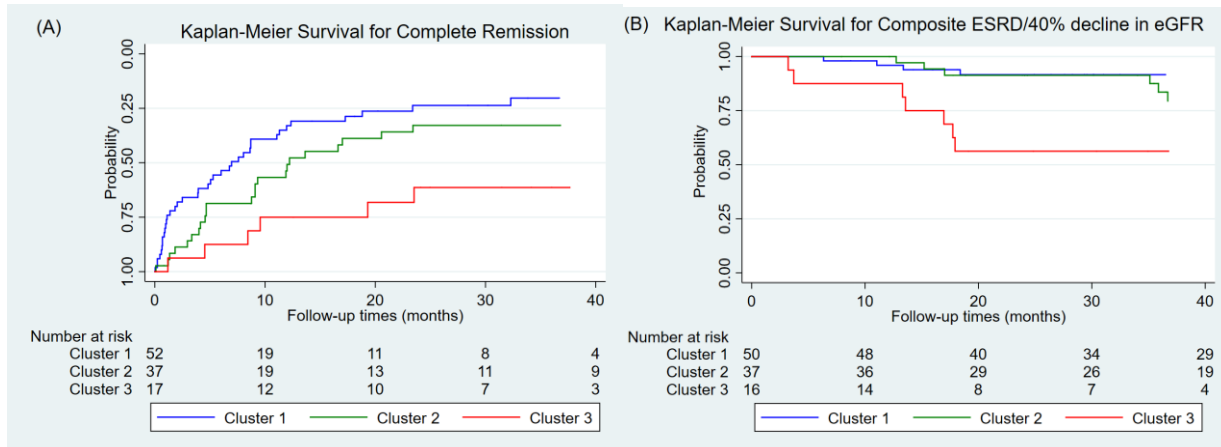


Figure 1: Overall strategy to identify non-invasive urinary markers for tissue-derived molecular patient subgroups.

Figure 2: Unadjusted Kaplan Meier curves by cluster membership for complete remission of proteinuria from time of screening, p-value 0.002 (A), and composite of ESRD/40% drop in eGFR from baseline, p-value 0.007 (B).



*Patients reaching endpoint prior to at risk entry were excluded from the analysis

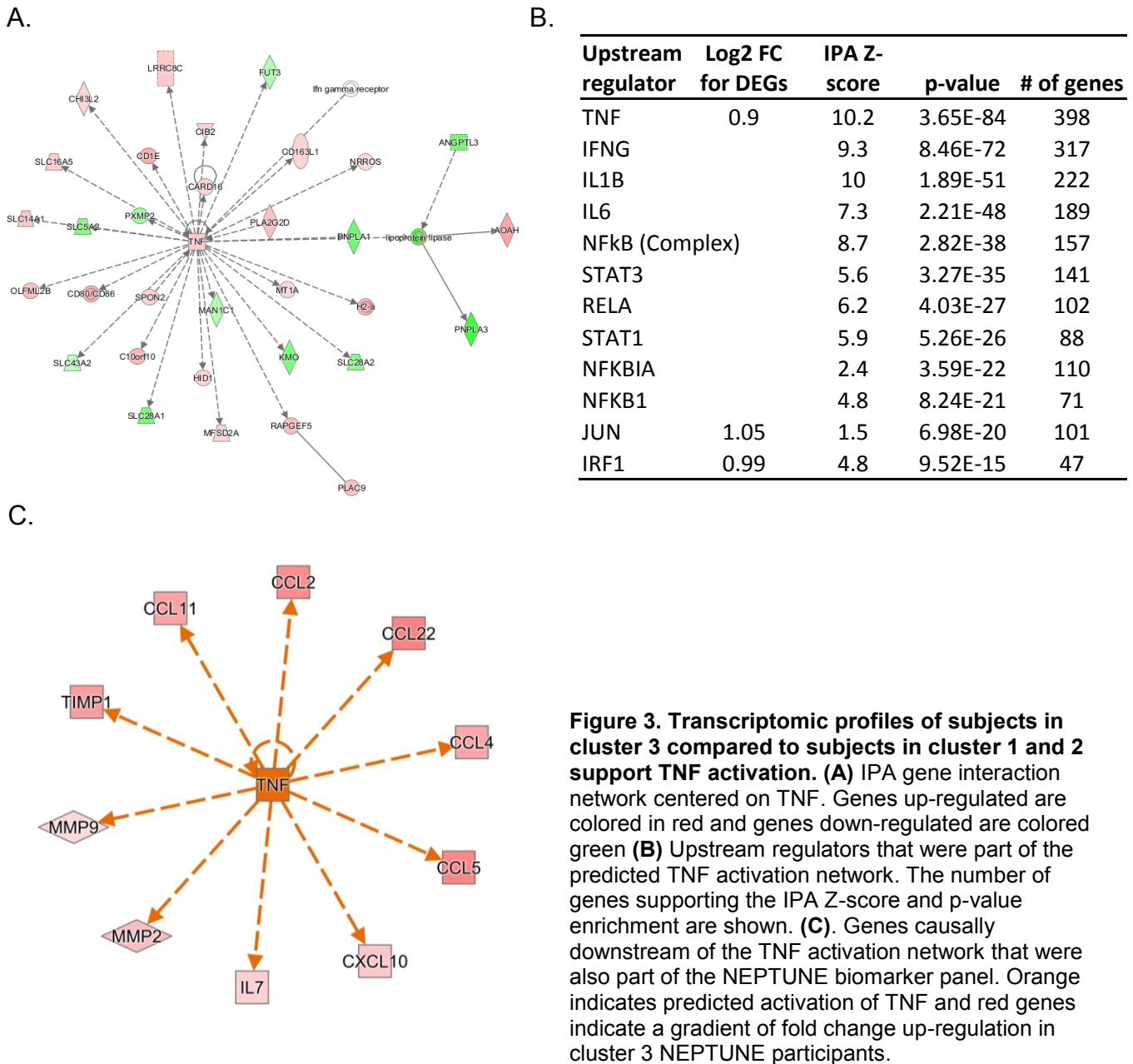


Figure 4: Distribution of TNF patient scores across all profiled participants and by cluster membership.

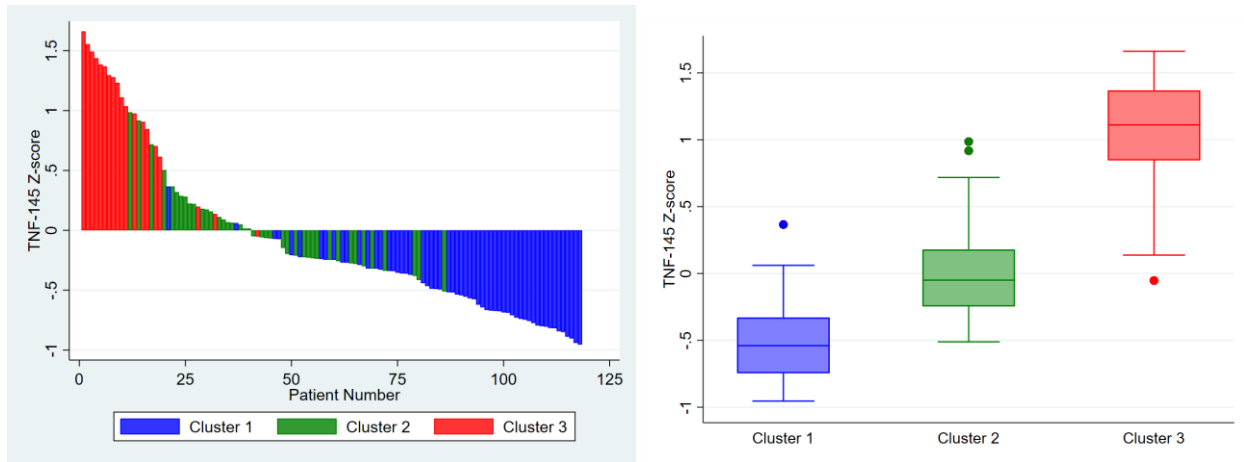


Figure 5: TNF alpha activation was correlated with interstitial fibrosis.

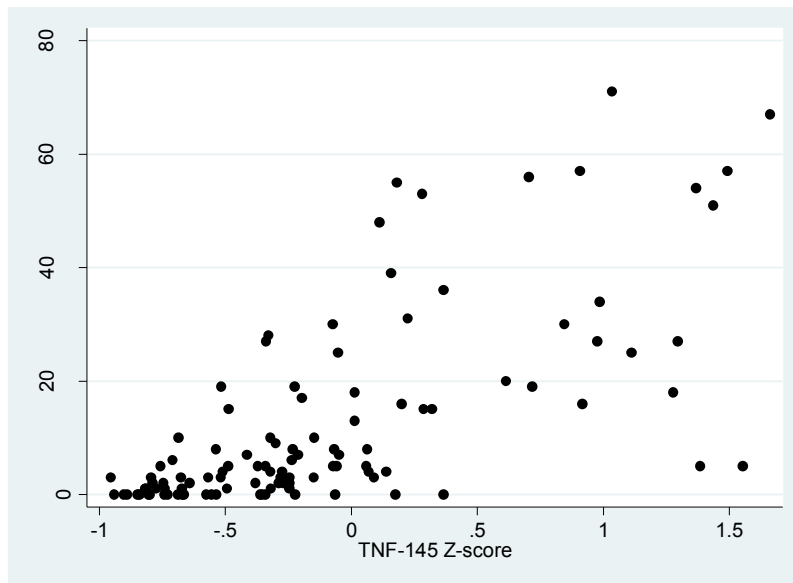


Figure 6. Urinary inflammatory biomarkers correlate with TNF activation score. (A) A prioritization schema was applied to identify biomarkers with the most reliable intra-renal mRNA and urine proteomic profile correlations. **(B)** Intra-renal and urine biomarker profile correlation plots in subjects with MCD or FSGS for CCL2 (left panel) and TIMP1 (right panel). **(C)** TNF activation score plotted against urine biomarker profiles for MCP1 and TIMP1.

A. Causal Genes

| Downstream of TNF >75% of samples activation | | | |
|--|------------------|------|---------|
| | in dynamic range | R2 | p-value |
| CCL2 | Yes | 0.34 | <0.001 |
| TIMP1 | Yes | 0.25 | <0.001 |
| CXCL10 | Yes | 0.18 | <0.001 |
| CCL4 | Yes | 0.03 | 0.2 |
| CCL11 | Yes | 0.01 | 0.5 |
| CCL5 | Yes | 0.00 | 0.7 |
| CCL22 | Yes | 0.00 | 0.7 |
| MMP2 | No | 0.18 | <0.001 |
| TNF | No | 0.07 | 0.04 |
| MMP9 | No | 0.04 | 0.1 |
| IL17 | No | 0.03 | 0.2 |

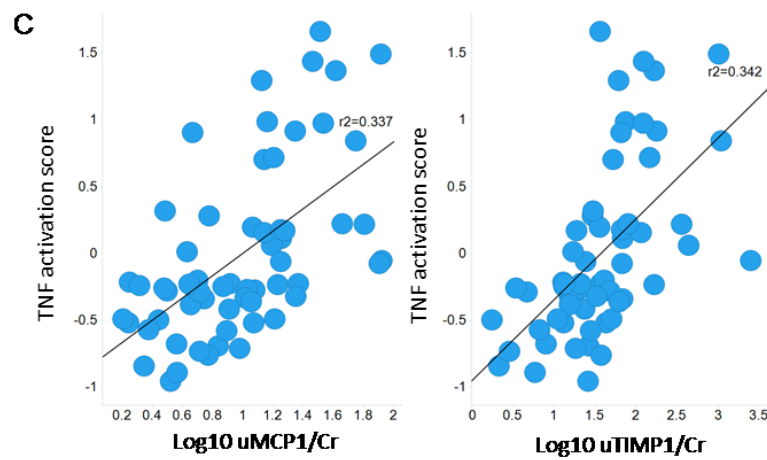
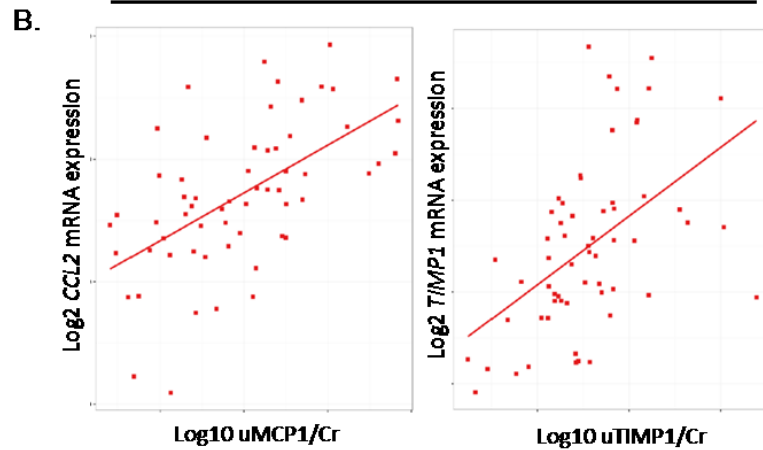


Table 1: Baseline characteristics of participants by gene expression cluster. Continuous, normally distributed variables are presented as mean (SD). Continuous, non-normally distributed variables are presented as median (IQR). Categorical variables are presented as n(%).

| | All (N = 123) | Cluster 1 (N = 62) | Cluster 2 (N = 42) | Cluster 3 (N = 19) | p-value |
|--------------------------------------|------------------|-----------------------|-----------------------|-----------------------|---------|
| Age (years) | 29 (22) | 17 (16) | 39 (23) | 44 (18) | <0.001 |
| Black Race | 40 (34%) | 18 (31%) | 12(30%) | 10 (53%) | 0.17 |
| Female | 41 (35%) | 22 (38%) | 18 (44%) | 6 (32%) | 0.31 |
| FSGS | 67 (57%) | 22 (38%) | 30 (73%) | 15 (79%) | <0.001 |
| Disease Duration (months) | 4 (1, 26) | 4.5 (1.5, 17.5) | 6.5 (2, 52) | 1.0 (0, 20) | 0.06 |
| eGFR (mL/min/1.73m ²) | 88 (36) | 108 (31) | 79 (28) | 45 (20) | <0.001 |
| UPCR (mg/mg) | 1.2 (0.3, 3.5) | 0.7 (0.1, 2.7) | 1.5 (0.7, 3.6) | 2.4 (1.5, 4.6) | 0.01 |
| % IF | 5 (1, 19) | 1 (0, 5) | 9 (4, 19) | 27 (18, 56) | <0.001 |
| On RAAS Blockade | 67 (57%) | 24 (41%) | 31 (76%) | 12 (63%) | 0.003 |
| On IST | 60 (51%) | 37 (64%) | 18 (44%) | 5 (26%) | 0.01 |

*eGFR: estimated glomerular filtration rate; MCD: Minimal Change Disease; FSGS: Focal Segmental Glomerulosclerosis; UPCR: Urine protein to creatinine ratio; IF: Interstitial Fibrosis; RAAS: Renin-angiotensin Aldosterone System; IST: Immunosuppressive Therapy

Table 2: Generalized Estimating Equations (GEE) of eGFR (mL/min/1.73m²) after the baseline visit. Separate models for cluster membership and TNF activation score as primary predictors of interest.

| | Predictor | Univariable Model | | Multivariable Model* | |
|-------------------------------|----------------------|----------------------|---------|----------------------|---------|
| | | Coefficient (95% CI) | p-value | Coefficient (95% CI) | p-value |
| Model 1: Cluster Membership | Cluster 1 | Ref | | Ref. | |
| | Cluster 2 | -28 (-17, -38) | <0.001 | -9 (0.5, -19) | 0.06 |
| | Cluster 3 | -55 (-40, -70) | <0.001 | -19 (-5, -32) | 0.006 |
| Model 2: TNF activation Score | TNF Activation Score | -31 (-23, -40) | <0.001 | -12 (-4, -19) | 0.002 |

*Multivariable model adjusted for age, sex, race, diagnosis, baseline eGFR, UPCR and time.

Table 3: Logistic Regression of positive TNF activation score

| Luminex (n=61, 23 Events) | Model 1 c-statistic 0.86 PPV 79% correctly classified 80% | | Model 2 c-statistic 0.79 PPV 67% Correctly classified 71% | | Model 3 c-statistic 0.86 PPV 82% Correctly Classified 80% | | Mode 4 c-statistic 0.91 PPV 81% Correctly Classified 84% | |
|------------------------------|--|---------|---|---------|--|---------|--|---------|
| | OR | P-value | OR | P-value | OR | P-value | OR | p-value |
| Log2(uTIMP1/Creat) | 2.23 | 0.001 | | | 1.92 | 0.03 | | |
| Log2(uMCP1/Creat) | | | 2.23 | 0.001 | 1.29 | 0.43 | | |
| Age | | | | | | | 0.99 | 0.76 |
| UPCR | | | | | | | 1.99 | 0.02 |
| eGFR | | | | | | | 0.94 | 0.001 |

Supplementary Materials

Supplemental Table 1: Baseline characteristics of ERCB participants by gene expression cluster.

Continuous, normally distributed variables are presented as mean (SD). Continuous, non-normally distributed variables are presented as median (IQR). Categorical variables are presented as n(%).

| | All (N = 30) | Cluster 1 (N = 5) | Cluster 2 (N = 19) | Cluster 3 (N = 6) | p-value (Clust. 3 vs 1+2) |
|--------------------------------------|-----------------|----------------------|-----------------------|----------------------|---------------------------------|
| Age (years) | Mean (SD) | 47(15) | 39(18) | 48(21) | 0.55 |
| Female | N (%) | 4 (80%) | 8 (42%) | 2 (33%) | 0.65 |
| FSGS | N (%) | 3 (60%) | 9 (47%) | 5 (83%) | 0.19 |
| eGFR (mL/min/1.73m ²) | Mean (SD) | 71 (45) | 100 (30) | 35 (17) | <0.001 |

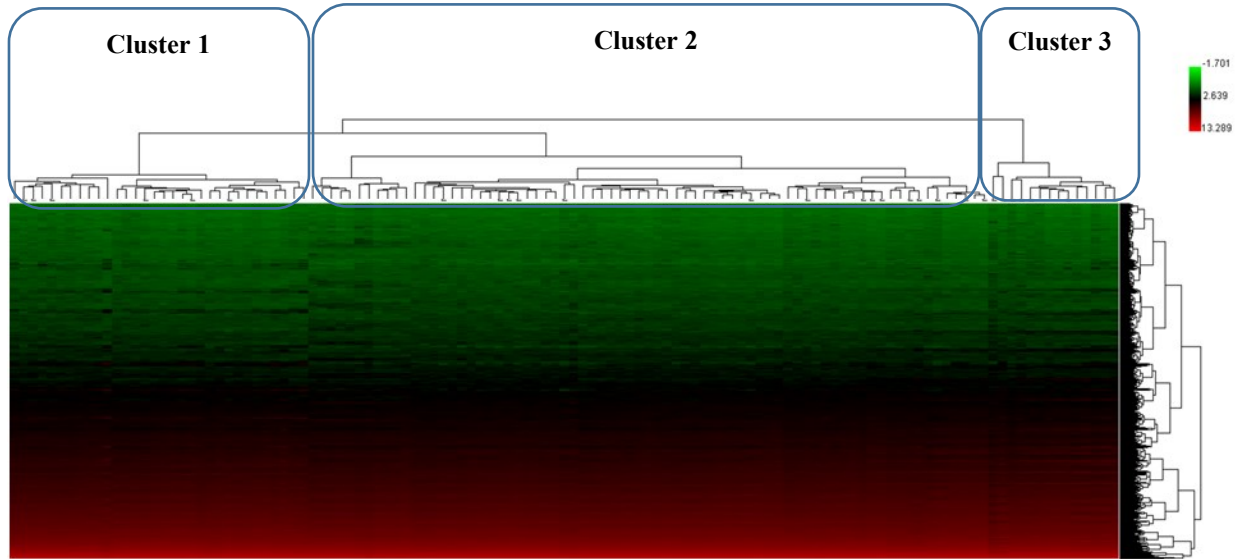
*eGFR: estimated glomerular filtration rate; MCD: Minimal Change Disease; FSGS: Focal Segmental Glomerulosclerosis.

Supplemental Table 2: TNF-regulated genes contributing to the TNF activation score

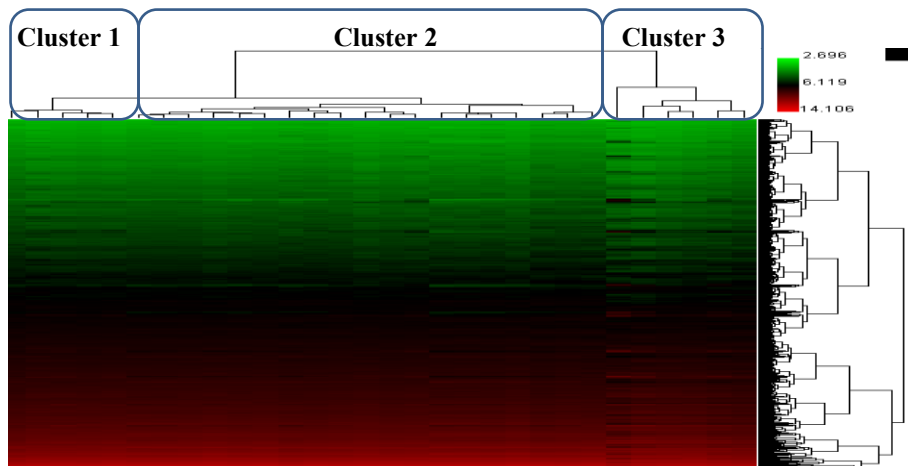
| Entrez ID | Gene Symbol | Entrez ID | Gene Symbol | Entrez ID | Gene Symbol | Entrez ID | Gene Symbol | Entrez ID | Gene Symbol |
|-----------|-------------|-----------|-------------|-----------|-------------|-----------|-------------|-----------|-------------|
| 12 | SERPINA3 | 1436 | CSF1R | 3575 | IL7R | 5359 | PLSCR1 | 7127 | TNFAIP2 |
| 31 | ACACA | 1520 | CTSS | 3587 | IL10RA | 5696 | PSMB8 | 7128 | TNFAIP3 |
| 154 | ADRB2 | 1524 | CX3CR1 | 3606 | IL18 | 5698 | PSMB9 | 7130 | TNFAIP6 |
| 165 | AEBP1 | 1536 | CYBB | 3624 | INHBA | 5699 | PSMB10 | 7133 | TNFRSF1B |
| 240 | ALOX5 | 1545 | CYP1B1 | 3627 | CXCL10 | 5788 | PTPRC | 7412 | VCAM1 |
| 241 | ALOX5AP | 1634 | DCN | 3659 | IRF1 | 5806 | PTX3 | 7424 | VEGFC |
| 330 | BIRC3 | 1848 | DUSP6 | 3676 | ITGA4 | 6036 | RNASE2 | 7474 | WNT5A |
| 355 | FAS | 1903 | S1PR3 | 3678 | ITGA5 | 6279 | S100A8 | 7852 | CXCR4 |
| 567 | B2M | 1906 | EDN1 | 3683 | ITGAL | 6288 | SAA1 | 7980 | TFPI2 |
| 597 | BCL2A1 | 1958 | EGR1 | 3684 | ITGAM | 6347 | CCL2 | 8870 | IER3 |
| 602 | BCL3 | 1999 | ELF3 | 3685 | ITGAV | 6351 | CCL4 | 9021 | SOCS3 |
| 629 | CFB | 2113 | ETS1 | 3689 | ITGB2 | 6352 | CCL5 | 9023 | CH25H |
| 718 | C3 | 2213 | FCGR2B | 3690 | ITGB3 | 6356 | CCL11 | 9180 | OSMR |
| 834 | CASP1 | 2335 | FN1 | 3694 | ITGB6 | 6363 | CCL19 | 9536 | PTGES |
| 837 | CASP4 | 2353 | FOS | 3725 | JUN | 6364 | CCL20 | 9636 | ISG15 |
| 920 | CD4 | 2634 | GBP2 | 3726 | JUNB | 6367 | CCL22 | 10512 | SEMA3C |
| 929 | CD14 | 2833 | CXCR3 | 3934 | LCN2 | 6372 | CXCL6 | 10537 | UBD |
| 942 | CD86 | 2920 | CXCL2 | 4050 | LTB | 6401 | SELE | 10563 | CXCL13 |
| 952 | CD38 | 3082 | HGF | 4071 | TM4SF1 | 6403 | SELP | 11221 | DUSP10 |
| 958 | CD40 | 3091 | HIF1A | 4233 | MET | 6422 | SFRP1 | 25816 | TNFAIP8 |
| 960 | CD44 | 3133 | HLA-E | 4313 | MMP2 | 6772 | STAT1 | 26298 | EHF |
| 1009 | CDH11 | 3383 | ICAM1 | 4318 | MMP9 | 6868 | ADAM17 | 51284 | TLR7 |
| 1026 | CDKN1A | 3428 | IFI16 | 4323 | MMP14 | 6890 | TAP1 | 58191 | CXCL16 |
| 1051 | CEBPB | 3459 | IFNGR1 | 4609 | MYC | 7040 | TGFB1 | 64332 | NFKBIZ |
| 1191 | CLU | 3489 | IGFBP6 | 4688 | NCF2 | 7052 | TGM2 | 79689 | STEAP4 |
| 1233 | CCR4 | 3554 | IL1R1 | 5054 | SERPINE1 | 7076 | TIMP1 | 112464 | PRKCDBP |
| 1236 | CCR7 | 3563 | IL3RA | 5284 | PIGR | 7097 | TLR2 | 114548 | NLRP3 |
| 1316 | KLF6 | 3566 | IL4R | 5328 | PLAU | 7099 | TLR4 | 414062 | CCL3L3 |
| 1435 | CSF1 | 3574 | IL7 | 5329 | PLAUR | 7124 | TNF | 729230 | CCR2 |

Supplemental Figure 1: Cluster dendrogram of (A) NEPTUNE MCD and FSGS participants based on kidney biopsy tubulointerstitial gene expression data and (B) ERCB MCD and FSGS participants based on kidney biopsy tubulointerstitial gene expression data.

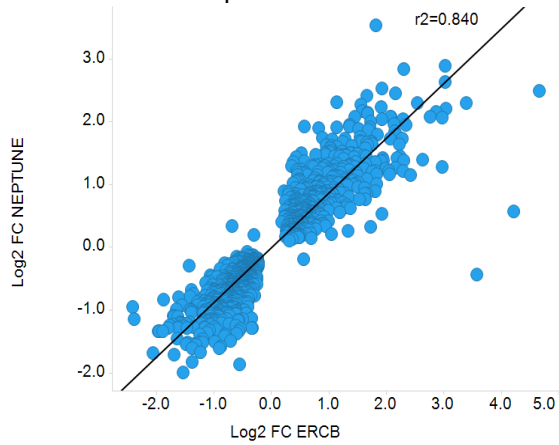
A.



B.



Supplemental Figure 2. Log2 fold changes are presented for each dataset. Genes significantly differentially expressed (1,259 genes, $q < 0.05$) in samples from cluster 3 patients for both NEPTUNE and ERCB cohorts are presented.



References:

1. V. D. D'Agati *et al.*, Association of histologic variants in FSGS clinical trial with presenting features and outcomes. *Clin J Am Soc Nephrol* **8**, 399-406 (2013).
2. R. M. Lombel, E. M. Hodson, D. S. Gipson, O. Kidney Disease: Improving Global, Treatment of steroid-resistant nephrotic syndrome in children: new guidelines from KDIGO. *Pediatr Nephrol* **28**, 409-414 (2013).
3. R. M. Lombel, D. S. Gipson, E. M. Hodson, O. Kidney Disease: Improving Global, Treatment of steroid-sensitive nephrotic syndrome: new guidelines from KDIGO. *Pediatr Nephrol* **28**, 415-426 (2013).
4. M. S. Joy *et al.*, Phase 1 trial of adalimumab in Focal Segmental Glomerulosclerosis (FSGS): II. Report of the FONT (Novel Therapies for Resistant FSGS) study group. *Am J Kidney Dis* **55**, 50-60 (2010).
5. L. Zand, R. J. Glasscock, A. S. De Vriese, S. Sethi, F. C. Fervenza, What are we missing in the clinical trials of focal segmental glomerulosclerosis? *Nephrol Dial Transplant* **32**, i14-i21 (2017).
6. P. Ravani, E. Bertelli, S. Gill, G. M. Ghiggeri, Clinical trials in minimal change disease. *Nephrol Dial Transplant* **32**, i7-i13 (2017).
7. F. S. Collins, Reengineering translational science: the time is right. *Sci Transl Med* **3**, 90cm17 (2011).
8. J. E. Wiggins *et al.*, NFkappaB promotes inflammation, coagulation, and fibrosis in the aging glomerulus. *Journal of the American Society of Nephrology : JASN* **21**, 587-597 (2010).
9. S. Martini *et al.*, Integrative biology identifies shared transcriptional networks in CKD. *J Am Soc Nephrol* **25**, 2559-2572 (2014).
10. H. Schmid *et al.*, Modular activation of nuclear factor-kappaB transcriptional programs in human diabetic nephropathy. *Diabetes* **55**, 2993-3003 (2006).
11. J. Tao *et al.*, JAK-STAT signaling is activated in the kidney and peripheral blood cells of patients with focal segmental glomerulosclerosis. *Kidney Int*, (2018).
12. C. F. Ware, The TNF Superfamily-2008. *Cytokine & growth factor reviews* **19**, 183-186 (2008).
13. M. Jaattela, Biologic activities and mechanisms of action of tumor necrosis factor-alpha/cachectin. *Laboratory investigation; a journal of technical methods and pathology* **64**, 724-742 (1991).
14. T. Hernandez, T. N. Mayadas, Immunoregulatory role of TNFalpha in inflammatory kidney diseases. *Kidney international* **76**, 262-276 (2009).
15. L. Baud, B. Fouqueray, C. Philippe, A. Amrani, Tumor necrosis factor alpha and mesangial cells. *Kidney international* **41**, 600-603 (1992).
16. E. T. McCarthy *et al.*, TNF-alpha increases albumin permeability of isolated rat glomeruli through the generation of superoxide. *Journal of the American Society of Nephrology : JASN* **9**, 433-438 (1998).
17. L. Le Berre *et al.*, Renal macrophage activation and Th2 polarization precedes the development of nephrotic syndrome in Buffalo/Mna rats. *Kidney international* **68**, 2079-2090 (2005).
18. A. Bakr *et al.*, Tumor necrosis factor-alpha production from mononuclear cells in nephrotic syndrome. *Pediatric nephrology* **18**, 516-520 (2003).
19. A. Peyser *et al.*, Follow-up of phase I trial of adalimumab and rosiglitazone in FSGS: III. Report of the FONT study group. *BMC Nephrol* **11**, 2 (2010).
20. D. Raveh, O. Shemesh, Y. J. Ashkenazi, R. Winkler, V. Barak, Tumor necrosis factor-alpha blocking agent as a treatment for nephrotic syndrome. *Pediatr Nephrol* **19**, 1281-1284 (2004).
21. S. Ito *et al.*, Long-term remission of nephrotic syndrome with etanercept for concomitant juvenile idiopathic arthritis. *Pediatr Nephrol* **25**, 2175-2177 (2010).
22. L. H. Mariani *et al.*, Interstitial fibrosis scored on whole-slide digital imaging of kidney biopsies is a predictor of outcome in proteinuric glomerulopathies. *Nephrol Dial Transplant* **33**, 310-318 (2018).
23. L. Barisoni *et al.*, Digital pathology evaluation in the multicenter Nephrotic Syndrome Study Network (NEPTUNE). *Clin J Am Soc Nephrol* **8**, 1449-1459 (2013).
24. C. A. Gadegbeku *et al.*, Design of the Nephrotic Syndrome Study Network (NEPTUNE) to evaluate primary glomerular nephropathy by a multidisciplinary approach. *Kidney Int* **83**, 749-756 (2013).

25. Y. Yasuda, C. D. Cohen, A. Henger, M. Kretzler, D. N. A. B. C. European Renal c, Gene expression profiling analysis in nephrology: towards molecular definition of renal disease. *Clin Exp Nephrol* **10**, 91-98 (2006).
26. J. Y. Lai *et al.*, MicroRNA-21 in Glomerular Injury. *Journal of the American Society of Nephrology* **26**, 805-816 (2015).
27. H. Schmid *et al.*, Modular Activation of Nuclear Factor- κ B Transcriptional Programs in Human Diabetic Nephropathy. *Diabetes* **55**, 2993-3003 (2006).
28. C. D. Cohen, K. Frach, D. Schlondorff, M. Kretzler, Quantitative gene expression analysis in renal biopsies: a novel protocol for a high-throughput multicenter application. *Kidney Int* **61**, 133-140 (2002).
29. P. C. Grayson *et al.*, Metabolic pathways and immunometabolism in rare kidney diseases. *Ann Rheum Dis* **77**, 1226-1233 (2018).
30. N. L. Catlett *et al.*, Reverse causal reasoning: applying qualitative causal knowledge to the interpretation of high-throughput data. *BMC Bioinformatics* **14**, 340 (2013).